Sensitivity of tropical climate to low-level clouds in the NCEP climate forecast system

Zeng-Zhen Hu · Bohua Huang · Yu-Tai Hou · Wanqiu Wang · Fanglin Yang · Cristiana Stan · Edwin K. Schneider

Abstract In this work, we examine the sensitivity of tropical mean climate and seasonal cycle to low clouds and cloud liquid water path (CLWP) by prescribing them in the NCEP climate forecast system (CFS). It is found that the change of low cloud cover alone has a minor influence on the amount of net shortwave radiation reaching the surface and on the warm biases in the southeastern Atlantic. In experiments where CLWP is prescribed using observations, the mean climate in the tropics is improved significantly, implying that shortwave radiation absorption by CLWP is mainly responsible for reducing the excessive surface net shortwave radiation over the southern oceans in the CFS. Corresponding to large CLWP values in the southeastern oceans, the model generates large low cloud amounts. That results in a reduction of net shortwave radiation at the ocean surface and the warm biases in the sea surface temperature in the southeastern oceans. Meanwhile, the cold tongue and associated surface wind stress in the eastern oceans become stronger and more realistic. As a consequence of the overall improvement of the tropical mean climate, the seasonal cycle in the tropical Atlantic is also improved. Based on the results from these sensitivity experiments, we propose a model bias correction approach, in which CLWP is prescribed only in the southeastern Atlantic by using observed annual mean climatology of CLWP. It is shown that the warm biases in the southeastern Atlantic are largely eliminated, and the seasonal cycle in the tropical Atlantic Ocean is significantly improved. Prescribing CLWP in the CFS is then an effective interim technique to reduce model biases and to improve the simulation of seasonal cycle in the tropics.

Keywords Low cloud amount · Cloud liquid water path · NCEP climate forecast system · Tropical mean climate and seasonal cycle · Tropical Atlantic

Z.-Z. Hu · B. Huang · C. Stan · E. K. Schneider
Center for Ocean-Land-Atmosphere Studies, 4041 Powder Mill Road, Suite 302, Calverton, MD 20705, USA

Z.-Z. Hu (✉) · W. Wang
Climate Prediction Center, NCEP/NWS/NOAA, 5200 Auth Road (Suite 605), Camp Springs, MD 20746, USA
e-mail: Zeng-Zhen.Hu@noaa.gov

B. Huang · E. K. Schneider
Department of Atmospheric, Oceanic, and Earth Sciences, College of Science, George Mason University, 4400 University Drive, Fairfax, VA 22030, USA

Y.-T. Hou · F. Yang
Environmental Modeling Center, NCEP/NWS/NOAA, 5200 Auth Road, Camp Springs, MD 20746, USA

1 Introduction

Stratocumulus cloud decks in the southeastern Pacific and Atlantic Oceans have been documented by Klein and Hartmann (1993), Norris (1998), and Xie (2005). Climatologically, the daytime frequency of the existence of stratocumulus clouds reaches 30–70% in the southeastern tropical Pacific and Atlantic (Klein and Hartmann 1993; Norris 1998). The formation of the stratocumulus clouds is closely tied to the vertical thermal structure of the lower stratosphere. Cold ocean surface and a very stable lower troposphere, usually with temperature inversion, co-exist with a thin layer of stratocumulus clouds at the base of an inversion layer over a relatively shallow marine boundary layer (MBL) (Klein and Hartmann 1993; Tanimoto and Xie 2002; Wood and Bretherton 2006). The existence of these

stratocumulus clouds substantially reduces the downward shortwave radiation reaching the sea surface and cools the ocean surface, which reinforces the inversion stratification (Siebesma et al. 2004; Huang and Hu 2007). Recently, Clement et al. (2009) suggested that the positive feedback between low-level cloud and ocean surface temperature/atmospheric circulation in the northeast Pacific may play an important role in the local variability on decadal time scales. The occurrence and evolution of the stratocumulus clouds involve complicated dynamic and thermodynamic processes and feedbacks (Mitchell and Wallace 1992; Philander et al. 1996; Nigam 1997; Xie et al. 2007; Huang and Hu 2007). It is still a challenge to correctly simulate the occurrence and evolution of these stratocumulus clouds and their climate effects in state-of-the-art general circulation models (GCMs).

Underestimation of the amount of stratocumulus clouds over the tropical oceans is a common defect of contemporary coupled climate models (Huang et al. 2007; Hu et al. 2008a). Moreover, the underestimation of the amount of stratocumulus clouds seems to be tied to pronounced warm biases in the tropical eastern oceans (e.g., Neelin et al. 1992; Mechoso et al. 1995; Davey et al. 2002; Huang et al. 2007; Collins et al. 2006; Deser et al. 2006; Huang et al. 2007; Hu et al. 2008a). For example, warm biases can reach 4–5°C in the southeastern tropical Pacific and Atlantic in versions 2 and 3 of the Community Climate System Model (CCSM2 and CCSM3) (see Fig. 5 of Collins et al. 2006). Hu and Huang (2007) and Hu et al. (2008a) found that these biases can reduce climate prediction skill and may alter the southern subtropical variability modes in the tropical Atlantic. Thus, it is necessary to examine the impact of stratocumulus clouds on model systematic errors in order to reduce model biases and to enhance their ability in simulating and predicting climate variability and change.

Actually, efforts have been made to examine the role of stratocumulus clouds in the sea surface temperature (SST) in the tropical Pacific in coupled general circulation models (CGCMs). For example, Philander et al. (1996) suggested that low-level stratus clouds over cold water are crucial in the maintenance of tropical climate asymmetries and that there is a strong feedback between stratus clouds, SST, and lower atmosphere stability. They used the temperature difference between the sea surface and 850 hPa to parameterize the formation of low-level stratus clouds and found that introducing this stratocumulus parameterization into a GCM caused significant cooling in the tropical Pacific, especially in the southeastern Pacific. Ma et al. (1996) conducted two 2.5 year integrations using a CGCM: a control simulation in which the simulated amount of Peruvian stratocumulus clouds was unrealistically low, and an experiment in which constant overcast conditions (100%) were prescribed to persistently cover the ocean off

the Peruvian coast (10°S–30°S, 90°W to the South American coast). It was found that, beneath the prescribed cloud deck, SSTs were reduced by up to 5°K, as expected from decreased solar radiation reaching the surface. Later, Yu and Mechoso (1999) extended the work of Ma et al. (1996) by prescribing the regionally persistently idealized stratocumulus clouds in different seasons and by extending the integrations to 5 years with a modified version of the GCM of Ma et al. (1996). Compared with the corresponding control run without cloud modification, it was suggested that the idealized annual variations of Peruvian stratocumulus clouds contributed to a more realistic intensity, duration, and westward propagation of the seasonal development of the equatorial cold tongue.

Late, Gordon et al. (2000) conducted a set of 23-year integrations prescribing observation-based monthly climatologies of low clouds over open ocean in the Geophysical Fluid Dynamics Laboratory (GFDL) GCM. To isolate the impact of low clouds, fixed optical depths were specified in all (sensitivity and control) experiments. They found significant improvement in the simulated mean annual and seasonal climate of the tropical Pacific and a clear impact on the interannual variability through complex dynamic and thermodynamic processes. Gudgel et al. (2001) extended the work of Gordon et al. (2000) by employing an improved version of the GFDL CGCM and by conducting a set of 1 year forecasts of 1984–1993 with ten ensemble members in each forecast. In these forecast experiments, both the low cloud fraction and optical depth were replaced by observation-based interannually varying data over the global ocean only, or over the global ocean plus observation-based monthly climatologies over global or eastern/western hemisphere tropical land (15°S–15°N). It was demonstrated that the seasonal distribution of low-level clouds over both ocean and land influences the strength and position of the Walker circulation, and also affects the strength and phase of the El Niño-Southern Oscillation (ENSO). It was also suggested that a corrected distribution of low clouds in the model enhances the skill of predicting ENSO (Gudgel et al. 2001).

This study is complementary to our recent work in diagnosing the biases and prediction skill, as well as the most predictable patterns, of the climate forecast system (CFS) of the National Centers for Environmental Prediction (NCEP) in the tropical Atlantic (Huang and Hu 2007; Huang et al. 2007; Hu and Huang 2007; Hu et al. 2008a, b). Huang et al. (2007) and Hu et al. (2008a) found that the amplitude of warm SST biases in the southeastern Atlantic are comparable to those in the southeastern Pacific. These biases are associated with low hindcast skill and unrealistic simulation of the southern subtropical mode of variability in the southeastern Atlantic (Hu and Huang 2007; Hu et al. 2008b). Cloud–radiation–SST interaction processes play an

important role in model bias evolution as well as in anomalous climate events in the southeastern Atlantic (Huang et al. 2007; Huang and Hu 2007; Hu et al. 2008a). In this work, using the CFS, we examine the sensitivity of the tropical mean climate and seasonal cycle not only to the change of low cloud cover, but also to the change of cloud liquid water path (CLWP). Through these experiments, a scheme of model bias correction is proposed and its efficiency is tested. Another difference of this work compared with previous studies is that we focus on the tropical Atlantic Ocean. We believe that the cloud radiation effects may be equal or even more important in the Atlantic than those in the Pacific because the low clouds in the southeast cover a larger fraction of the total Atlantic basin than the Pacific (Norris 1998). The paper is organized as follows. Observation-based data, the model, and the experimental design are described in Sect. 2. The impacts of low cloud and CLWP modifications on tropical mean climate and seasonal cycle are examined in Sect. 3. Section 4 provides conclusions and discussion.

2 Observation-based data, model, and experimental design

2.1 Observation-based data

Observation-based monthly cloud coverage data used in this work were produced by the International Satellite Cloud Climatology Project (ISCCP). The datasets of global distribution of clouds and their properties were created by using a series of satellite radiance measurements (Rossow and Dueñas 2004). The low-, middle-, and high-level clouds are categorized as below 680 hPa, between 680 and 440 hPa, and above 440 hPa, respectively. The corresponding monthly net shortwave radiative fluxes at the surface were derived by using a complete radiative transfer model with input from surface and atmospheric observations and ISCCP cloud properties (Zhang et al. 2004). Both the cloud and radiation data are on a 2.5° × 2.5° grid and span from July 1983 to December 2004.

Besides traditional cloud cover, CLWP is also an important factor affecting the radiation budget at the surface. CLWP plays a role similar to cloud cover in affecting atmospheric dynamics primarily through latent heating and modulation of both shortwave and longwave radiative transfer. Spaceborne measurements of cloud liquid water are best determined by microwave instruments, which directly respond to the thermal emission of cloud droplets (Weng et al. 1997). Because the low-frequency microwave channels fully penetrate virtually all clouds, they can provide a direct measurement of the total liquid (but not solid) cloud condensate amount (O'Dell et al. 2008). In this work,

the CLWP data on a 1° × 1° grid, termed the University of Wisconsin (UWisc) climatology (O'Dell et al. 2008), are used. The data were derived from satellite-based passive microwave observations over the global oceans and based on a modern retrieval methodology applied consistently to the Special Sensor Microwave Imager, the Tropical Rainfall Measuring Mission Microwave Imager, and the Advanced Microwave Scanning Radiometer for Earth Observing System microwave sensors on eight different satellite platforms in January 1988–December 2007. It was noted that this climatology exhibits differences with previous observationally based climatologies and is found to be more consistent with the 40-year ECMWF reanalysis (Uppala et al. 2005) than the previous climatologies.

For comparison and validation, we use additional observation based data, such as the monthly mean data derived from the January 1948–December 2005 NCEP/NCAR re-analysis (Kalnay et al. 1996) and from the January 1950–December 2005 version 2 of the extended reconstruction of the SST analysis (ER-v2) on a 2° × 2° grid (Smith and Reynolds 2003). We also adopt the analyzed net surface heat flux data in January 1945–December 1993 from the Comprehensive Ocean-Atmosphere Data Set (COADS) on a 1° × 1° grid (Woodruff et al. 1987; da Silva et al. 1994). The COADS data are a collection of global marine surface observations taken primarily from ships and moored and drifting buoys. Analyzed precipitation data used in this study are on a 2.5° × 2.5° resolution grid in January 1979–December 2008, and are a combination of satellite retrievals, in situ rain gauge stations, and atmospheric model products (Xie and Arkin 1996, 1997). For convenience, all these observation based data are referred to as observations in this work.

2.2 Coupled model: NCEP CFS

The ocean–atmosphere CGCM used in this work is the NCEP CFS (Wang et al. 2005; Saha et al. 2006), which was developed at NCEP and used at NCEP for operational seasonal climate predictions. For the atmospheric component, the horizontal resolution is T62 and there are total 64 vertical sigma levels with about 20 sigma levels below 650 hPa. The oceanic component is configured from the version 3 of the Modular Ocean Model of GFDL (Pacanowski and Griffies 1998). There are 40 levels vertically, with 27 in the upper 400 meters for the ocean model. The domain of the ocean model is from 74°S to 64°N with a horizontal grid of 1° × 1° poleward of 30°S and 30°N, and with gradually increased meridional resolution to 1/3° between 10°S and 10°N. The atmospheric and oceanic components are coupled by exchanging surface fluxes on a daily interval without flux adjustment.

Since we are specifically concerned with clouds in this study, the cloudiness and boundary layer (BL) parameterization schemes used in the CFS are briefly reviewed here. The cloudiness parameterization is based on the semi-empirical stratiform cloudiness parameterization of Xu and Randall (1996). In this scheme, the primary predictor is the large-scale condensate (cloud water and cloud ice) mixing, and the large-scale relative humidity and cumulus mass flux are the secondary predictors. The cloud amount varies exponentially with the large-scale average condensate mixing ratio, and is also a function of large-scale relative humidity and the intensity of convection circulations (Xu and Randall 1996). In addition, the cloud condensate is a prognostic quantity found from a simple cloud microphysics parameterization and diagnostically determines the fractional cloud cover used for radiation calculations (Hou et al. 2002; Saha et al. 2006). Another important factor for the forming of low clouds is the formation of a MBL. The CFS adopts the nonlocal BL vertical diffusion scheme (Hong and Pan 1996). In this scheme, the turbulent diffusivity coefficients are calculated from a prescribed profile shape as a function of BL heights and scale parameters derived from similarity requirements (Hong and Pan 1996).

In the model output, besides the 3-dimensional clouds, clouds are also divided into four categories according to vertical extent: high, middle, low, and BLs, without considering overlapping. The BL clouds are defined as the clouds located within the lowest 10% of the total atmosphere mass. The other three layers are divided vertically between pressure levels. Over the regions between the equator and 45°, low clouds are referred to those above the BL cloud layer but below 650 hPa, middle clouds are between 350 and 650 hPa, and high clouds are above 350 hPa. Over the regions poleward of 45°, a linear change is used in these boundaries to simulate the 'squeezing' of the troposphere with the lowering of the tropopause. At the poles, the boundary decreases to 550 hPa between high and middle clouds and 750 hPa between middle and low clouds (Hu et al. 2008a).

It is clear that the low clouds in the CFS are not exactly the same as that in ISCCP. The former refers to the clouds above the BL but below 650 hPa, while the later simply to those below 680 hPa. However, the sum of low clouds and BL clouds from the CFS output, redefined as the CFS low clouds, may overestimate the actual low clouds in the CFS due to double counting of the overlapping part of low and BL clouds. But, Hu et al. (2008a) pointed out that the redefined low clouds in the CFS did not change the fact that the low clouds were underestimated in the tropical oceans compared with ISCCP. Furthermore, in ISCCP, only low-level clouds not being covered by higher clouds are counted. Therefore, given the same cloud distribution, low-level cloud fraction should be greater in the CFS definition

than in ISCCP. The difference in the cloud definitions only reduces the amplitudes of the low cloud underestimation over the tropical oceans in the CFS, and thus does not change the conclusion that the CFS low cloud amount is persistently low compared with that in ISCCP as pointed out by Hu et al. (2008a).

The solar radiative transfer model used in the CFS includes parameterizations of absorptions by various gases, clouds, and aerosols, as well as scattering by clouds, aerosols, and gas molecules (Hou et al. 2002). In cloud related radiation calculation, water vapor amount and CLWP are the two major factors used in absorption and cloud optical depth computation, respectively.

2.3 Experimental design

To investigate the impact of prescribed low-level cloud cover and CLWP on tropical climate in the CFS, a set of coupled integrations were conducted (see Table 1). First, the model was integrated for 101 years with the initial conditions (IC) from ocean–atmosphere analysis for January 1, 1985. In this experiment, we used the same version of the CFS as Wang et al. (2005) and Saha et al. (2006), which is referred to as CONTROL. By analyzing a similar experiment, it has been demonstrated that the CFS reproduces most features of the leading modes of variability in the tropical Atlantic and their associated physical processes well (Hu et al. 2008b), although the SST was overestimated and the low clouds were underestimated in the southeastern Atlantic Ocean (Hu et al. 2008a).

In order to prescribe the vertical structure of low clouds, we first examined the 3-dimensional cloud data of the CFS. It was found that, for the global zonal average in the tropics (30°S–30°N), the majority of the low cloud in the CFS occurs in a layer between 650 and 750 hPa (bottom panel of Fig. 4 of Hu et al. 2009). These clouds, however, are located in a layer higher than the observed low clouds, because the averaged top pressure of the low clouds in ISCCP is in a range of 750–870 hPa (top panel of Fig. 4 of Hu et al. 2009). Furthermore, the top of the low clouds is generally higher over land than over oceans in ISCCP. On average, the top of the observed low clouds is below 810 hPa over oceans, and below 750 hPa over land. This result confirmed the speculation of Hu et al. (2008a) that low clouds are generated in a higher layer in the CFS than in the real world. It also implies that majority of prescribed low clouds over tropical oceans should be in a layer between 810 hPa and the surface. In the experiments described in the following, the majority of prescribed low clouds is set around 850 hPa.

In addition, further analyses show significant correlations between the simulated total low-cloud amount and the cloud cover in different levels of the lower troposphere in

Table 1 Experiments

Experiment name	Experiment description	Length of the integration and initial condition
CONTROL	No modification for clouds	101 years; January 1985
LCA1	Model global low clouds replaced by ISCCP climatological low clouds	5 years; January 1985
LCA2	Similar to LCA1, but replaced by ISCCP monthly low clouds	21 years; January 1984
CLWP1	Model low cloud portion of CLWP over global oceans is modified by adding observed monthly low cloud CLWP	20 years; January 1988
CLWP2	Similar to CLWP1, but modified only in the southeastern Atlantic	20 years; January 1988
CORRECTION	Similar to CLWP2, but modified by using observed annual mean climatology of CLWP in the southeastern Atlantic	50 years; January 1988

the CFS (not shown). This provides a physical basis for the modification of cloud cover in the lower troposphere in the CFS by using the observation-based total low-cloud amount through statistical approaches. Based on these diagnostic results, the vertical distribution of cloud amount in the layers between surface and 650 hPa is prescribed by the following equation:

$$\mathrm{CFS_{cloud}}(z) = \alpha * \mathrm{ISCCP_{lowcloud}} * \cos(\beta) \qquad (1)$$

where $\beta = \frac{\pi}{2}\frac{Pm-Pz}{Pm-Pt}$. Pz is the pressure in layer "z" in hPa. Pt and Pm are the pressures of the top and middle layers with cloud prescribed, respectively. According to the diagnostic results, we use following parameter values: Pt = 650 hPa, Pm = 850 hPa, and $\alpha = 1.0$ here. We assume the maximum at 850 hPa, which is consistent with recent work of Wu et al. (2009). By examining multi-sensor cloud height observations, they found that zonal mean cloud top heights are mostly between 1 and 2 km. Only the clouds in the layers between about 970 and 650 hPa are replaced by the ISCCP low clouds through using the above formula. For a few layers around 970 and 650 hPa, a blending technique is used to mix the CFS clouds and the ISCCP low clouds.

Based on the above formula, we design two experiments to test the impact of prescribed low cloud amount on the tropical climate. One uses the global climatological low cloud amount of ISCCP to replace the CFS clouds, which is referred to as LCA1 hereafter. The other uses the global monthly low clouds of ISCCP in January 1984–December 2004 to replace the CFS clouds and is referred to as LCA2. In LCA2, the monthly low clouds of ISCCP are first interpolated into daily data prior to being input into the model. The integration is 5 years from IC of January 1985 for LCA1, and 21 years from IC of January 1984 for LCA2.

Besides cloud amount, CLWP is another important factor in affecting the radiation. To examine the impact of CLWP, we conduct two experiments (CLWP1, CLWP2). In these experiments, the monthly data of CLWP for 1988–2007 from O'Dell et al. (2008) are prescribed over oceans. The seasonal mean climatologies of CLWP are shown in Fig. 1 (left panels). The analyzed CLWP is the vertical

integration of cloud liquid water content in the whole atmosphere column. To specify the low cloud portion of CLWP in the model from the total CLWP, we have to make some assumptions about the low cloud portion of CLWP and its vertical distribution. In this work, the low cloud portion of CLWP is defined as the production of CLWP of the whole column and the ratio of the monthly mean climatology of low cloud amount to the monthly mean climatology of total cloud amounts of ISCCP (right panels of Fig. 1). There are regional maxima of CLWP in the southeastern Pacific and Atlantic (left panels of Fig. 1), and the low cloud portions of CLWP enhance the maxima in these regions (right panels of Fig. 1). O'Dell et al. (2008) argued that the CLWP values are more accurate in the southeastern Pacific and Atlantic, largely covered by stratocumulus clouds, because these regions rarely have precipitation and icy clouds present. The accurate values of CLWP provide a solid basis for testing the hypnosis that the simulation of low clouds in these regions is one of major sources of the warm biases (Huang et al. 2007; Hu et al. 2008a).

In CLWP1 and CLWP2, similar to LCA2, the low cloud portion of observed monthly CLWP over the oceans is used to build vertical profiles of cloud using Eq. 1 and interpolated temporally into daily data prior to inputting into the model. In the vertical expansion using Eq. 1, $\alpha = 0.0824$ is adopted in order to keep the accumulation of the vertically interpolated CLWP between the surface and 650 hPa equal to the low cloud portion of the observed CLWP. To isolate the impact of large low cloud amount bias associated with the portion of CLWP, and based on the amplitude of the shortwave biases (Fig. 2a), we use spatial weights, which are defined as (shortwave bias in W/m^2 − 30)/60 (Fig. 2b) where positive, and zero otherwise. The global weights are used in CLWP1 (Fig. 2b), and the weights are equal to zero, except in the southeastern Atlantic Ocean for CLWP2 (Fig. 2c). Figure 2e and f are the mean weighted low cloud portion of observed CLWP used in the two experiments, which are defined as the values in Fig. 2d times the values in Fig. 2b and c, respectively. The weighted low cloud

Fig. 1 Seasonal mean climatology of CLWP (*left panels*) and the low cloud portion of CLWP (*right panels*), which is defined as the product of CLWP of the whole column and the ratio of monthly mean climatology of low cloud amounts to monthly mean climatology of total cloud amounts of ISCCP. The contour intervals are 20 g/m² for the *left panels* and 10 g/m² for the *right panels*
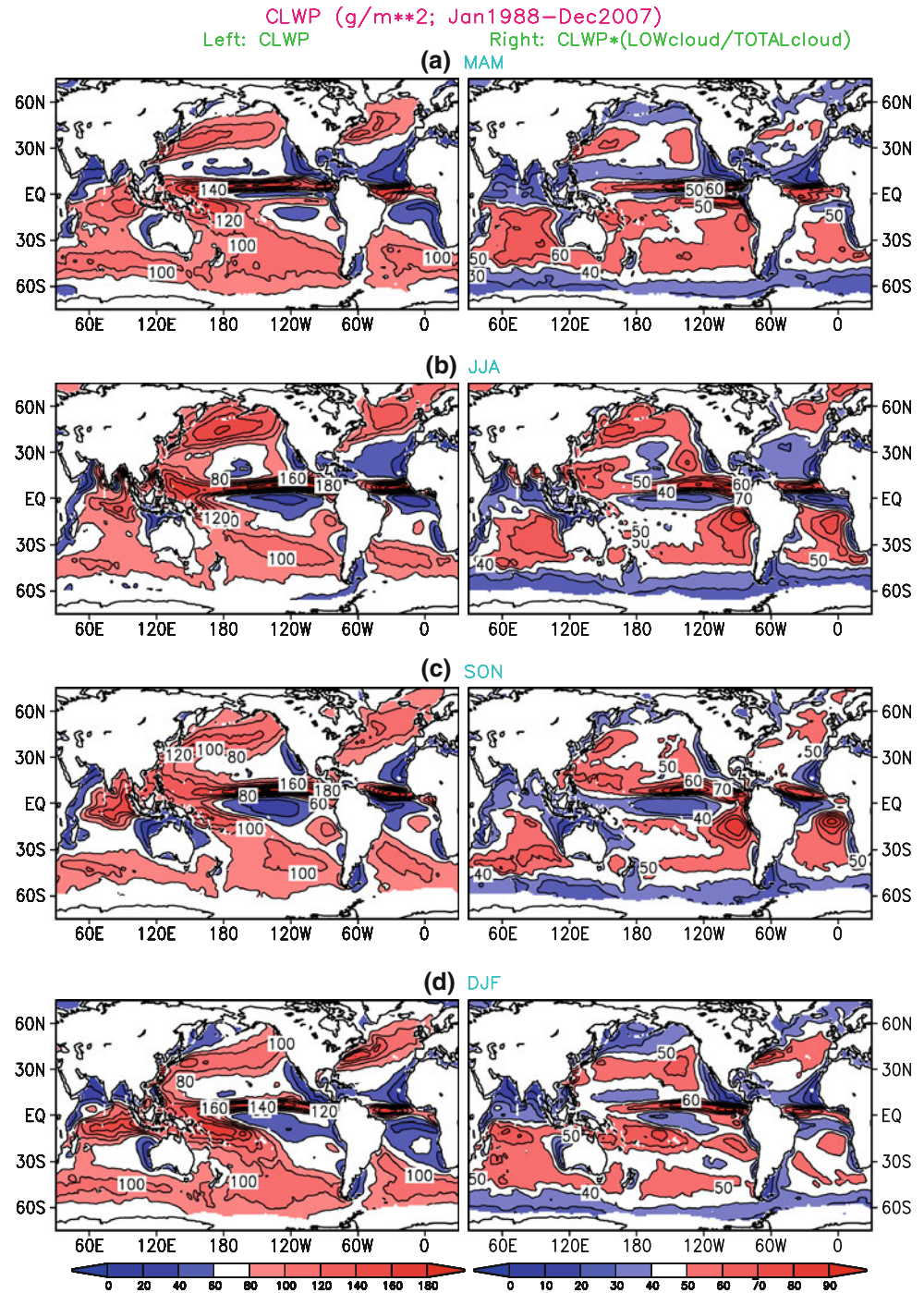

portion of observed CLWP is added into the model generated CLWP in the layers between the surface and 650 hPa, instead of replacing the model values as in LCA1 and LCA2. Using addition instead of replacement is due to the fact that the spatial weighted low-cloud portion of CLWP (Fig. 2e, f) is concentrated in some regions instead of the whole globe. The two experiments are integrated 20 years from IC of January 1988 (Table 1).

Based on the results of CLWP1 and CLWP2, we propose a scheme to eliminate the model biases by prescribing

climatological CLWP in the model. To test the scheme, we conduct another experiment (CORRECTION), which is similar to CLWP2 (only the CLWP in the southeastern Atlantic is prescribed), but uses annual mean climatology of observed CLWP rather than monthly values. CORRECTION is integrated 50 years from IC of January 1988 (Table 1). The sensitivity of tropical mean climate and the seasonal cycle to low cloud cover and the low cloud portion of CLWP is examined qualitatively using these experiments.

Fig. 2 a is the difference of mean net shortwave radiation (SW) at the surface between the CFS CONTROL and COADS. **b** is the weight used in the experiment "CLWP1", calculated mainly based on the equation "(SW bias − 30)/60". The SW bias is the difference shown in **a**. **c** is the weight used in the CLWP2 and CORRECTION experiments. **d** is the annual mean of the low cloud portion of CLWP. **e** and **f** are the results of weights in **b** and **c** multiplying **d**, respectively. The contour intervals are 20 W/m^2 in **a**, 0.2 in **b** and **c**, and 10 g/m^2 in **d**, and 20 g/m^2 in **e** and **f**
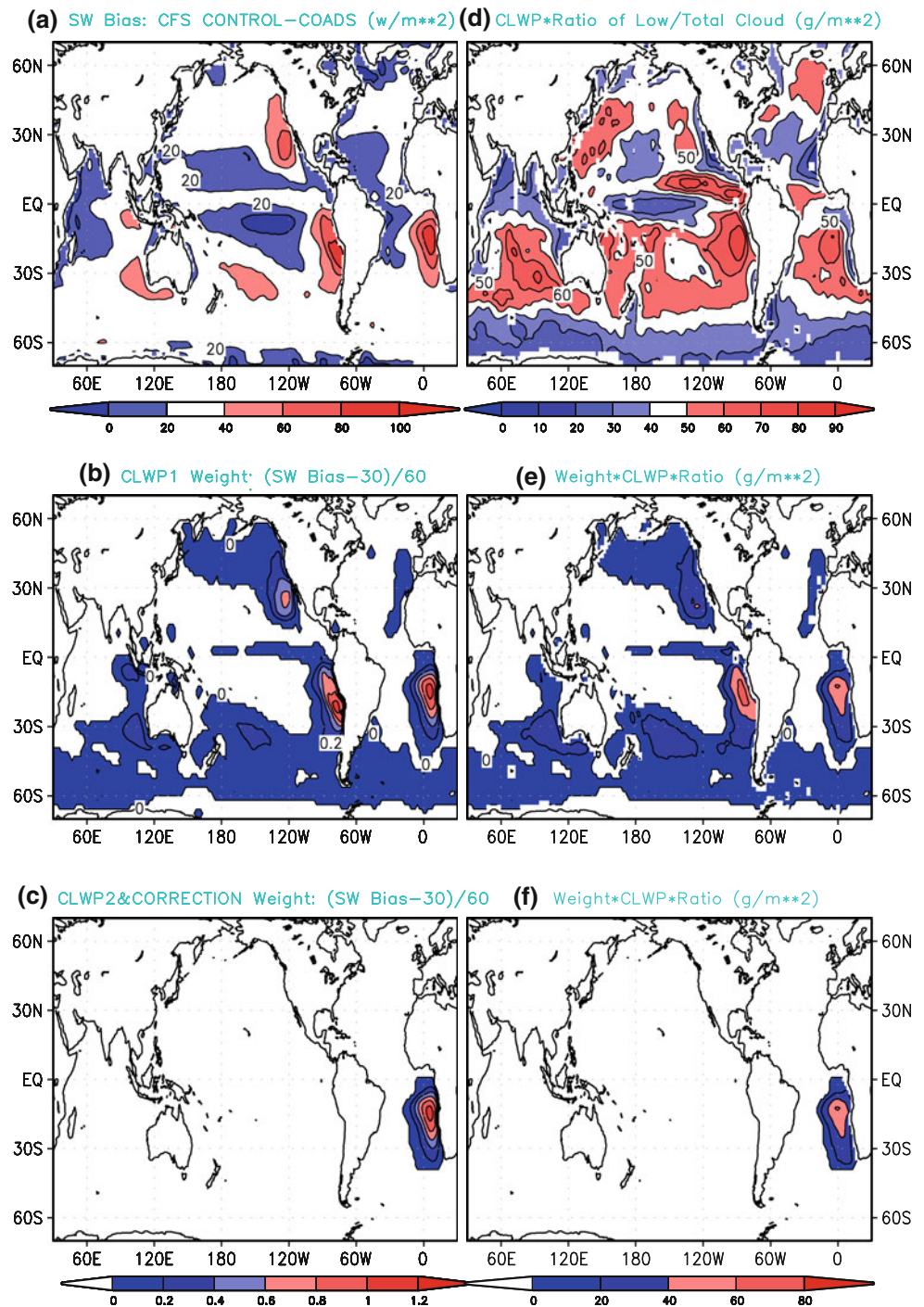
3 Impact of low cloud on tropical mean climate

3.1 Impact of low cloud cover

To examine the impact of low cloud cover modification on tropical mean climate, we focus on the tropical Atlantic Ocean. Figure 3 shows the mean low cloud amount, as well as mean and difference of net shortwave radiation at the surface in observations, CONTROL, and LCA2. As indicated by Hu et al. (2008a, b), although the seasonal variations of the low clouds are reasonably well simulated in the southeastern Atlantic Ocean, CFS underestimates the mean low clouds by about 25% (Fig. 3a–c, g), which is connected to the warm biases there. On the other hand, the mean low cloud amount in the whole tropical Atlantic Ocean and the interannual variation in the southeastern Atlantic Ocean are almost perfectly presented in LCA2 (Fig. 3a, c, g), as well as in LCA1 (not shown), which is a

significant improvement compared with CONTROL
(Fig. 3b, g). This demonstrates that a realistic 3-dimensional low cloud distribution is successfully prescribed in
the CFS by using Eq. 1.

Nevertheless, the improved low cloud cover only has a
minor influence on the amount of net shortwave radiation
reaching the surface (Fig. 3d–f) in the southeastern
Atlantic. This result suggests that low cloud cover plays a
secondary role in blocking and absorbing the radiation in
the radiation parameterization of the CFS. The absorption
and reflection of shortwave radiation by clouds mainly

depends on optical depth which is largely determined by
cloud liquid water content (Hou et al. 2002), which is
confirmed by the results in next subsection.

3.2 Impact of CLWP

Recently, we examined CLWP in the CFS, and compared it
with ERA40 reanalysis (Uppala et al. 2005), ISCCP, and
UWisc (O'Dell et al. 2008) analyses. It was found that
there are tremendous differences among these reanalyses
and analyses. ERA40 largely overestimates CLWP

Fig. 3 *Left column* mean cloud
amount in observations (ISCCP)
(**a**), CONTROL (**b**), and LCA2
(**c**). *Right column* net shortwave
radiation at the surface for
observation (COADS) (**d**), the
differences of CONTROL–
COADS (**d**) and LCA2–
CONTROL (**e**). *Bottom* regional
averaged monthly low cloud
amount in ISCCP (*solid*), LCA2
(*dashed*), and CONTROL (*dot*).
The averaged region is the
square in **a**–**c**. Contour interval
is 5% in **a**–**c**, 10 W/m² in **d**–**f**
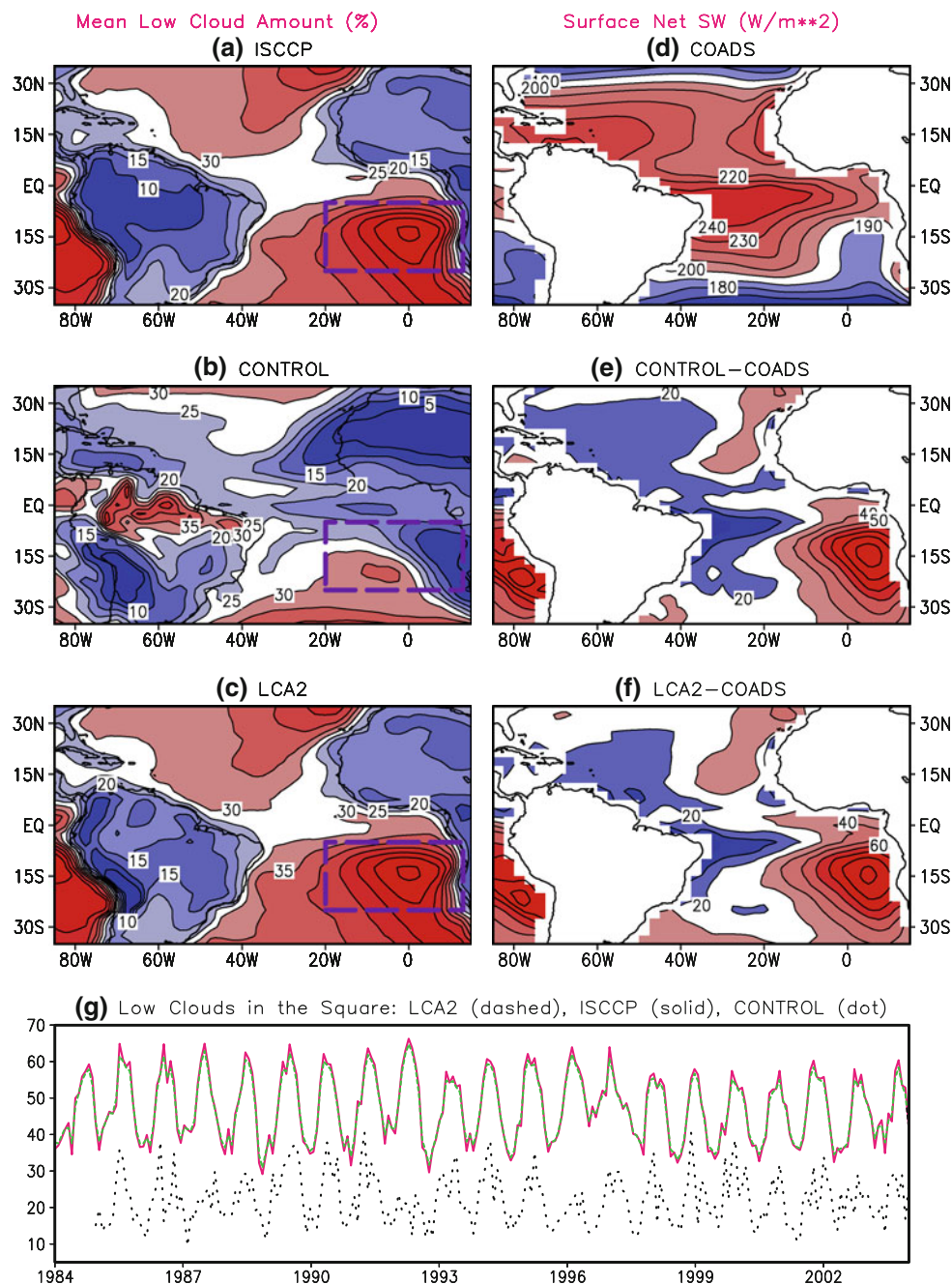
Fig. 4 *Left column* mean low cloud amount in observations (ISCCP) (**a**), CONTROL (**b**), CLWP1 (**c**), CLWP2 (**d**), and CORRECTION (**e**). *Right column* difference of low cloud amount between CONTROL and ISCCP (**f**), between CLWP1 and ISCCP (**g**), between CLWP2 and ISCCP (**h**), between CORRECTION and ISCCP (**i**), and between CLWP1 and CONTROL (**j**). Contour interval is 10%
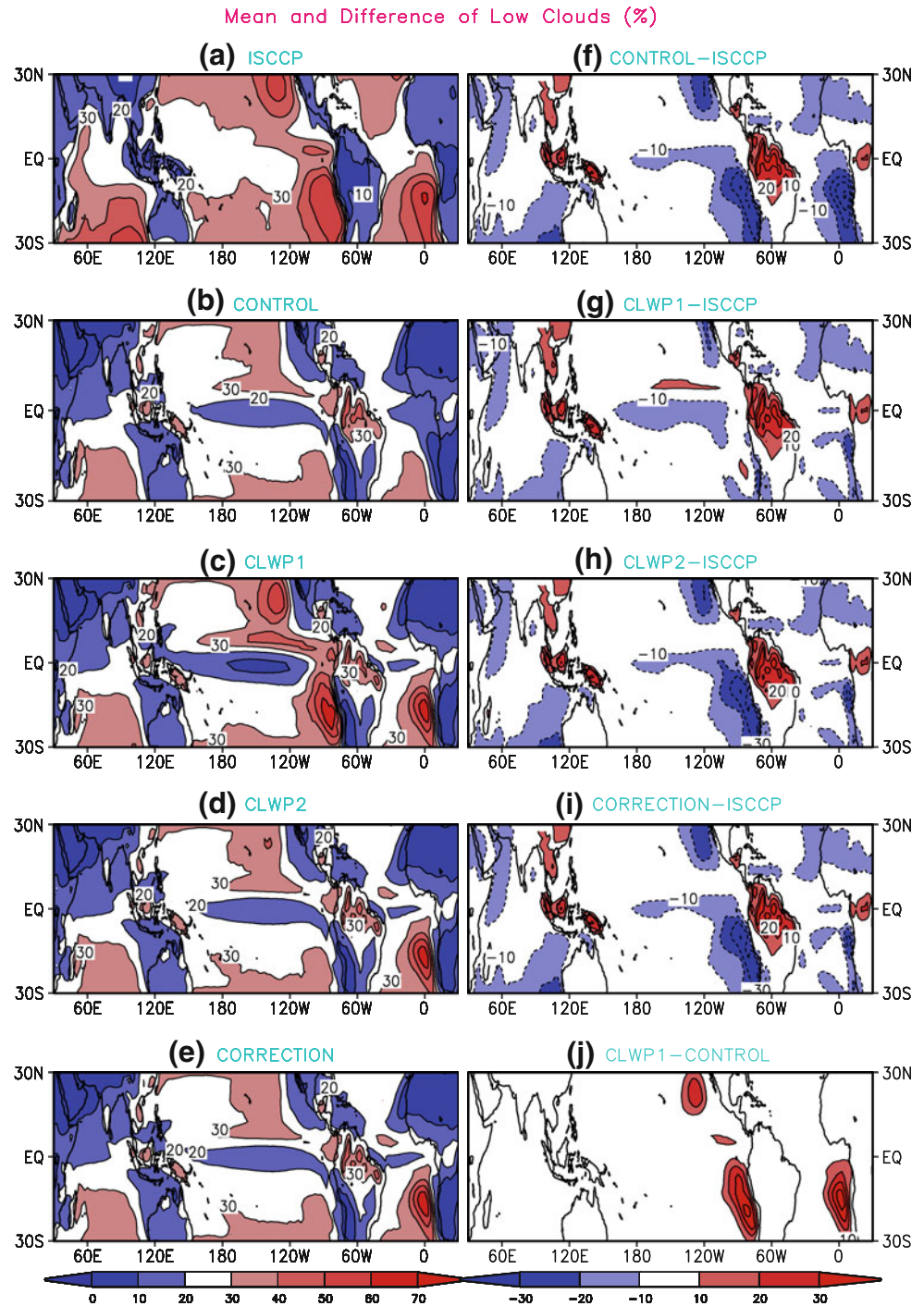
compared with the CFS and ISCCP as well as UWisc, which is consistent with the evidence that there are smaller warm biases and larger cold biases in the model of European Centre for Medium-Range Weather Forecasts than in the CFS (see Fig. 5 in Huang et al. 2007). That also suggests the importance of CLWP in correctly simulating mean climate, which is confirmed by the sensitivity experiments of CLWP1, CLWP2, and CORRECTION.

Compared with CONTROL, it is found that modifying CLWP can improve the simulation of low clouds (Fig. 4), because the low cloud in the CFS is diagnosed from cloud condensation. For example, when CLWP is prescribed globally in CLWP1, the biases of low clouds seen in CONTROL in the southeastern Pacific and Atlantic largely disappear (Fig. 4a–c, f, g, j). Similarly, when CLWP is modified only in the southeastern Atlantic in CLWP2 and

Fig. 5 *Left column* mean of net shortwave radiation at the ocean surface in observations (COADS) (**a**), CONTROL (**b**), CLWP1 (**c**), CLWP2 (**d**), and CORRECTION (**e**). *Right column* difference of net shortwave radiation at the ocean surface between CONTROL and COADS (**f**), between CLWP1 and CONTROL (**g**), between CLWP2 and CONTROL (**h**), and between CORRECTION and CONTROL (**i**). Contour interval is 20 W/m^2 in **a–e** and 10 W/m^2 in **f–i**
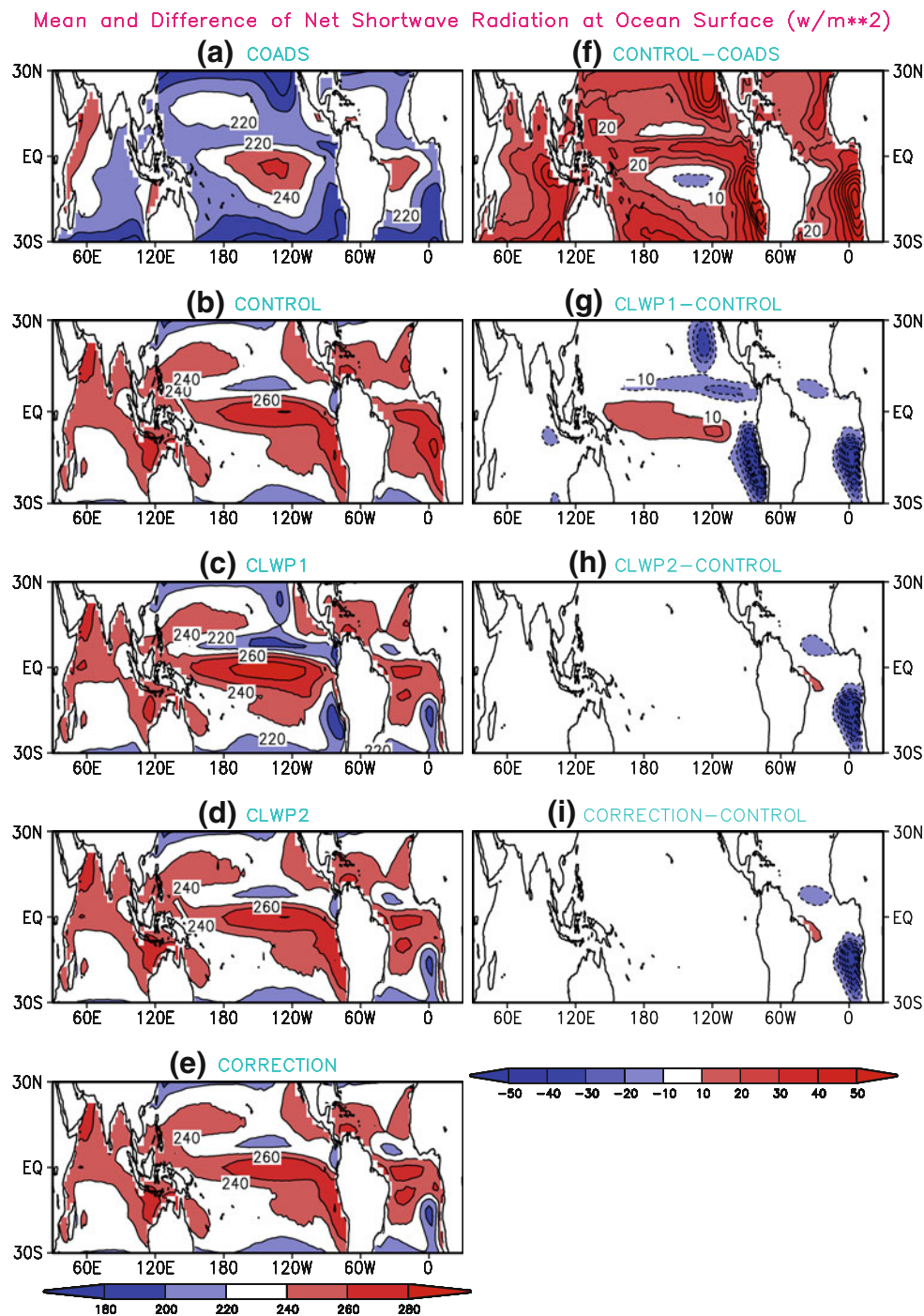
CORRECTION, the biases of low clouds in this region only are largely eliminated (Fig. 4d, e, h, i). The improvement of low clouds and CLWP consistently reduces the biases of net shortwave radiation at the ocean surface (Fig. 5). The largest changes in CLWP1 are in the southeastern Atlantic and Pacific Oceans (Fig. 5g), and in CLWP2 and CORRECTION only in the southeastern Atlantic (Fig. 5h, i), consistent with the corresponding modifications of low clouds (Fig. 4). The radiation change

results in cooling in the troposphere. For example, in the equatorial Atlantic, an obvious cooling tendency is observed in CLWP1, CLWP2, and CORRECTION compared with CONTROL (Fig. 6b–d). In contrast, there is almost no cooling tendency in LCA2 compared with CONTROL, except over the tropical Africa (Fig. 6a). These results suggest that shortwave radiation absorption by the CLWP is mainly responsible for reducing the excessive surface net shortwave radiation over the southern
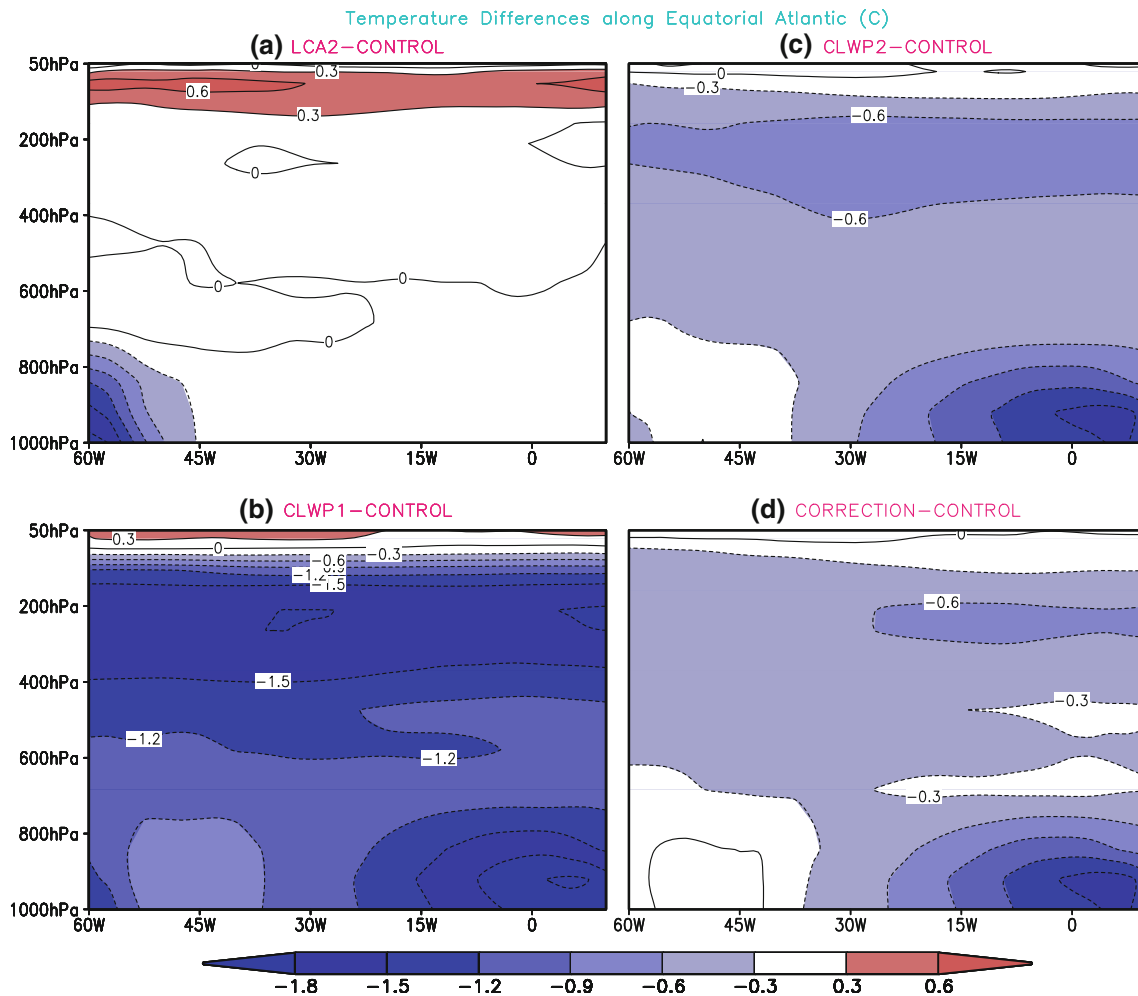
Fig. 6 Temperature difference of LCA2–CONTROL (**a**), CLWP1–CONTROL (**b**), CLWP2–CONTROL (**c**), and CORRECTION–CONTROL (**d**) along the equatorial Atlantic Ocean. Contour interval is 0.3°C

oceans in the CFS. The improved low cloud and shortwave radiation simulation improves the simulation of tropical mean climate and the seasonal cycle.

First, we see a clear improvement in the simulated SST and general increase of surface wind stress in the tropics (Fig. 7). A major problem in simulated tropical SST in the CFS as well as other state-of-the-art CGCMs is weak cold tongues in the eastern tropical Atlantic and Pacific Oceans. When CLWP is prescribed in both Pacific and Atlantic in CLWP1 (Fig. 7c), the cold tongue becomes much stronger and warm biases are reduced significantly in the eastern tropical oceans, and the easterly surface wind stress is enhanced along the equator in both oceans compared with CONTROL (Fig. 7c, f, g, j). However, when CLWP is prescribed only in the tropical Atlantic, improvement of SST and intensification of easterly surface wind stress are found only in the tropical Atlantic and changes in other regions are relatively small (Fig. 7d, e, f, h, i). These results indicate that improving CLWP in the CFS can

significantly reduce the warm biases of SST in the tropical Pacific and Atlantic Oceans.

Second, the change of CLWP also improves the simulation of SLP and general increase of easterly surface wind in the tropics (Fig. 8). Compared with observations, the SLP in CONTROL is overestimated in the western Pacific, particularly over the maritime continent, and underestimated in the central and eastern Pacific (Fig. 8a, b, f). There is a bias pattern: positive in the west and negative in the east (Fig. 8f). This bias pattern is due to the shift in the low pressure center from the maritime continent to central and eastern Pacific in CONTROL compared with observation. However, when CLWP is prescribed in both Pacific and Atlantic in CLWP1 (Fig. 8c), SLP is decreased over the western Pacific and increased in the eastern Pacific and Atlantic, generating a pattern with negative in the west and positive in the east compared with CONTROL (Fig. 8g). This partly offsets the biases in CONTROL (Fig. 8f) and improves the SLP simulations in the tropics. When CLWP

Fig. 7 *Left column* mean of SST (shading and contour) and surface wind stress (vector) in observations (NCEP/NCAR reanalysis and ERv2) (**a**), CONTROL (**b**), CLWP1 (**c**), CLWP2 (**d**), and CORRECTION (**e**). *Right column* difference of SST and surface wind stress between CONTROL and observations (**f**), between CLWP1 and observations (**g**), between CLWP2 and observations (**h**), between CORRECTION and observations (**i**), and between CLWP1 and CONTROL (**j**). Contour intervals of SST are 1°C in **a**–**e** and 0.5°C in **f**–**j**. The scales of the vectors are shown at the *top* of each column
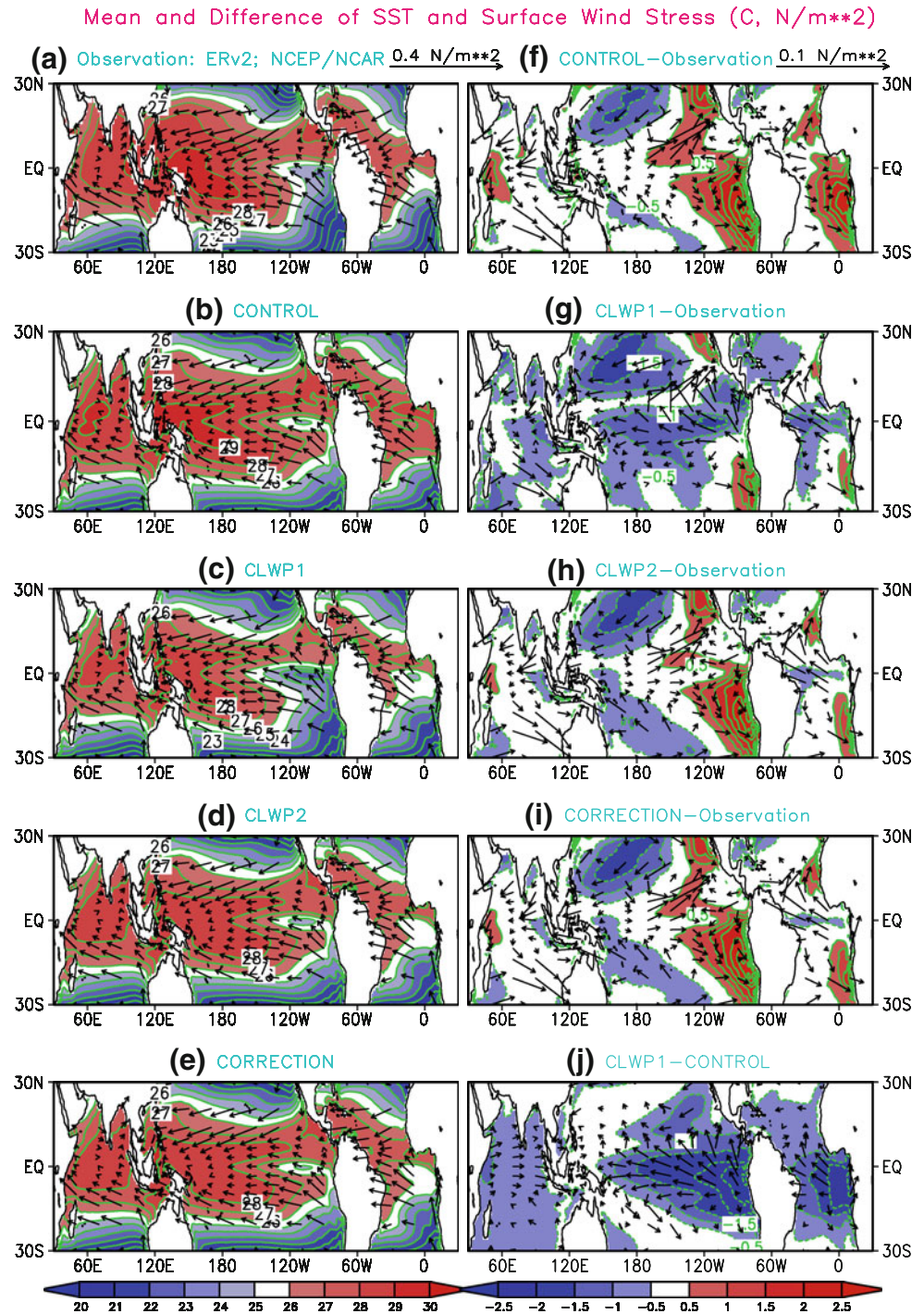
is prescribed only in the southeastern Atlantic in CLWP2 and CORRECTION, the SLP and surface wind are changed locally (Fig. 8d, e, h, i), consistent with the corresponding change in SST (Fig. 7h, i).

Third, prescribing CLWP not only improves the simulation of the mean climate, but also the seasonal cycle. Figure 9 shows the climatology of monthly mean SST and surface wind stress and the climatology of monthly mean departure of SST from its annual mean along the equatorial

Atlantic Ocean in the observations, CONTROL, CLWP1, CLWP2, and CORRECTION. Compared with the observations (Fig. 9a), it is found that associated with the warm bias is the underestimation of southerly wind stress along the African coast in CONTROL (Fig. 9b). When CLWP is prescribed in the Atlantic in CLWP1, CLWP2, and CORRECTION, the southerly wind stress initiates in February and increases in the later months (Fig. 9c–e), which is closer to the observations than CONTROL is

Fig. 8 *Left column* mean of sea level pressure (SLP) (shading and contour) and surface wind (vector) in observations (NCEP/NCAR reanalysis) (**a**), CONTROL (**b**), CLWP1 (**c**), CLWP2 (**d**), and CORRECTION (**e**). *Right column* difference of SLP and surface wind between CONTROL and observations (**f**), between CLWP1 and CONTROL (**g**), between CLWP2 and CONTROL (**h**), and between CORRECTION and CONTROL (**i**). Contour intervals of SLP are 2 hPa in **a–e** and 0.5 hPa in **f–i**. The scales of the vectors are shown at the *top* of each column
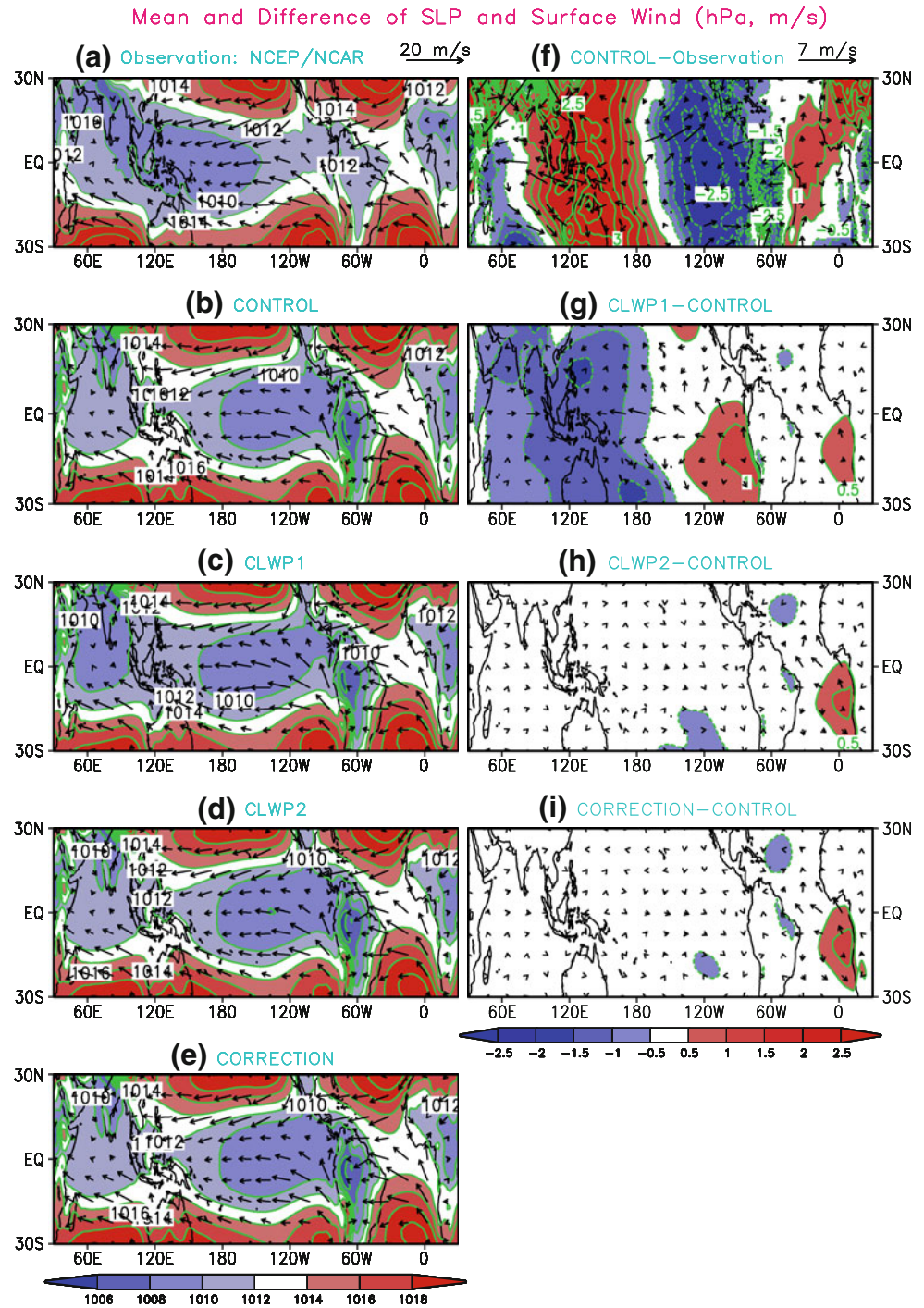
(Fig. 9a, b). Correspondingly, the seasonal cycle of SST is also improved. For example, the starting time of the seasonal warming is closer to the observations in CLWP1, CLWP2, and CORRECTION than in CONTROL. Moreover, the intensity of the SST annual cycle is enhanced and seasonal cold tongue enhancement becomes stronger after the mean cloud error is reduced. That is more consistent with the observations.

Moreover, the simulation of the inter-tropical convergence zone (ITCZ) in the tropical Atlantic is improved in CLWP1, CLWP2, and CORRECTION compared with CONTROL (Fig. 10). For example, there are double ITCZs in March–June in CONTROL, and the unrealistic southern branch of the ITCZ in 5°S–10°S (Fig. 10b) is largely eliminated in CLWP1, CLWP2, and CORRECTION (Fig. 10c–e). The northward movement of the ITCZ is
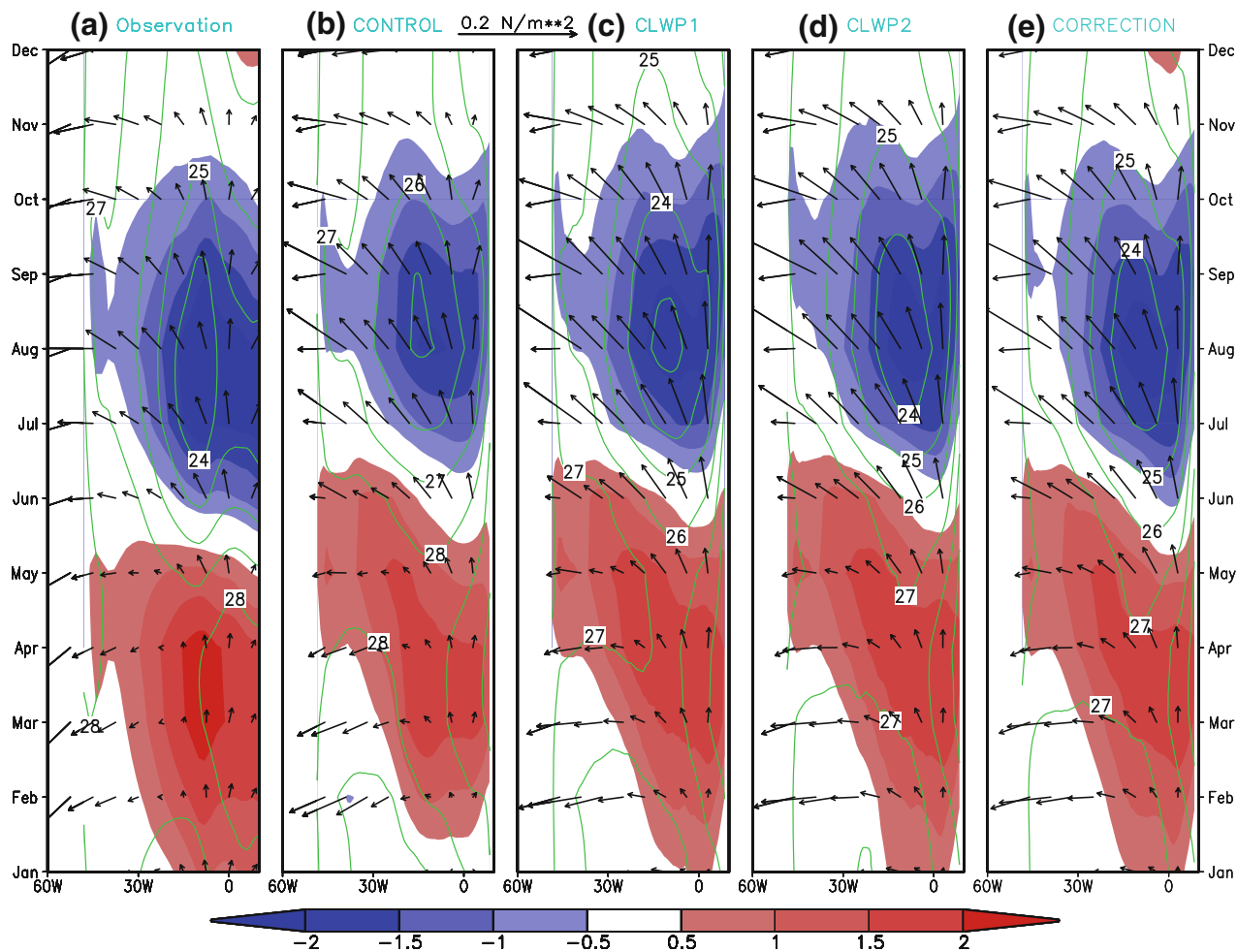
Fig. 9 Climatology of monthly mean of SST (contour) and surface wind stress (vector) and climatology of monthly mean departure of SST from its annual mean (shading) along the equatorial Atlantic Ocean in observation (NCEP/NCAR reanalysis and ERv2) (**a**), CONTROL (**b**), CLWP1 (**c**), CLWP2 (**d**), and CORRECTION (**e**). Contour interval is 1°C. The scale of the vector is shown at the *top* of the figure

steady in the observations (Fig. 10a), but is more abrupt in CONTROL due to a sudden enhancement of the southerly wind in June (see the thick line in Fig. 10b). In the CLWP prescribed experiments (CLWP1, CLWP2, CORREC-TION), the northward movement of the ITCZ is in between that of the observations and CONTROL (Fig. 10c–e). The improvement of the ITCZ is mainly associated with the enhancement of the southerly wind in the early part of the year. For example, the southerly wind along 10°S during January–May is stronger in the observations than in CON-TROL, and it is enhanced in CLWP1, CLWP2, and COR-RECTION compared with CONTROL (Fig. 10). The enhanced southerly wind does not favor the generation of ITCZ between 5° and 10°S during January–May (Fig. 10c–e). However, the overestimation of the ITCZ intensity in the boreal summer and early autumn in CONTROL, associated

with too strong southerlies, seems to be not improved much in the CLWP prescribed experiments (Fig. 10).

Overall, it is shown that using corrected CLWP in the CFS improves the simulations of the mean climate in the tropical oceans, including the centers of maximum low clouds and minimum of net shortwave radiation at the surface in the southeastern Pacific and Atlantic, and the cold tongue. We also note the improvement of the zonal SST gradient along the equatorial Atlantic Ocean. For example, the seasonal cycle of the SST slope is closer to the observation in CLWP1, CLWP2, and CORRECTION than in LCA2. The change in the mean climate makes the seasonal cycle in the tropical Atlantic Oceans improved. From the experiment of CORRECTION, we found the biases in the mean climate and seasonal cycle can be lar-gely eliminated by prescribing climatological mean

Fig. 10 Climatology of monthly mean of precipitation (shading) and v component of surface wind stress (vectors and contours) between 20°S and 20°N along 20°W in observation (NCEP/NCAR reanalysis and CAMP) (**a**), CONTROL (**b**), CLWP1 (**c**), CLWP2 (**d**), and CORRECTION (**e**). Zero contour line is omitted, *thick line* represents the contour of 0.02 N/m², and contour interval is 0.02 N/m². The scale of the vector is shown at the *bottom* of the *right column*

Monthly Mean of P and Surface Wind Stress v along 20W (mm/day, N/m**2)
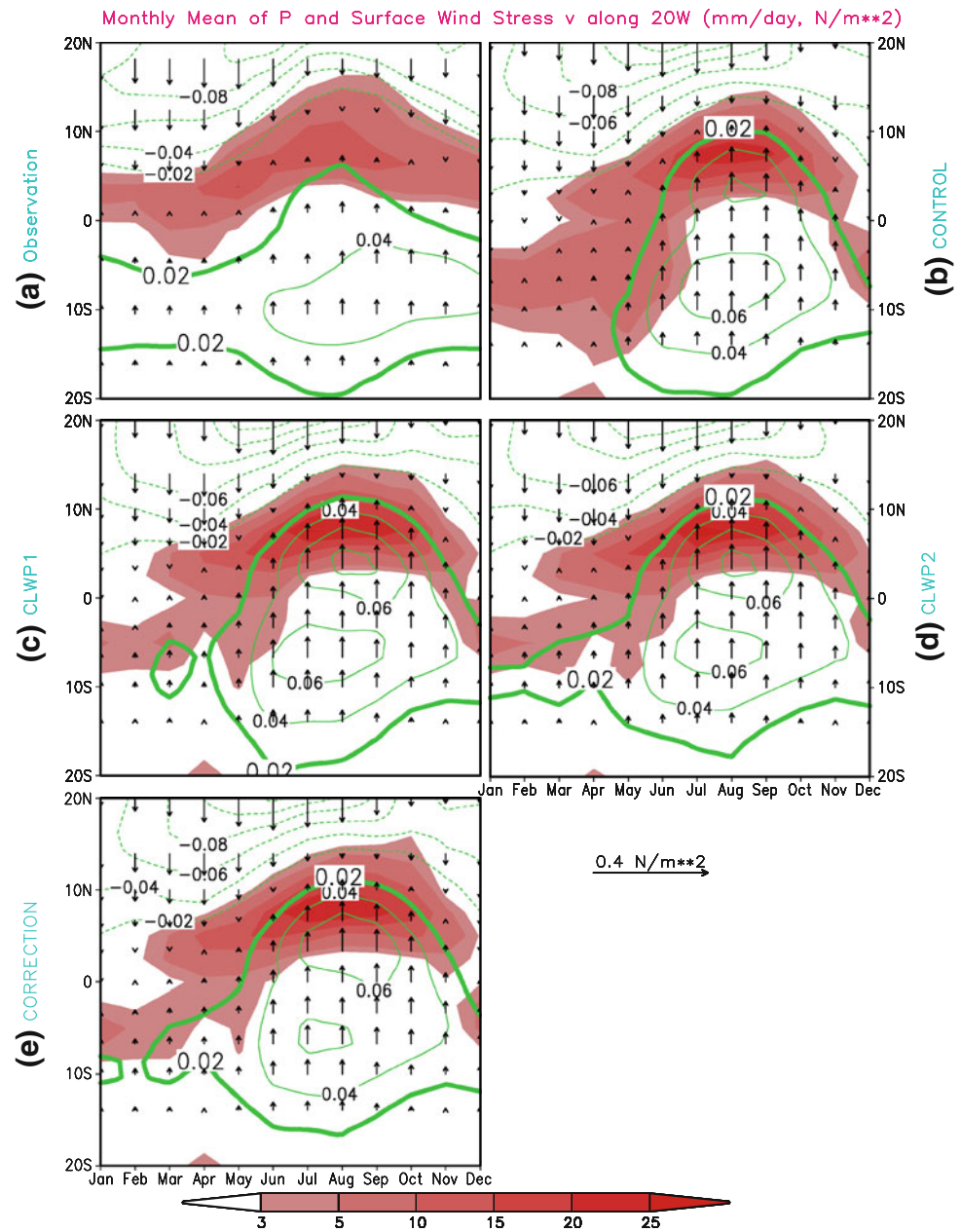
CLWP. The improvement of the seasonal cycle in CLWP1 and CLWP2 may be mainly due to the fact that the observed seasonal cycle of low clouds were prescribed. Nevertheless, the improvement of the seasonal cycle in CORRECTION, which seems to be from improved model dynamics, resulted from the reduced annual mean warm biases of SST.

4 Conclusion and discussion

In this work, we examined the sensitivity of tropical mean climate and seasonal cycle to low clouds and CLWP changes by prescribing them in the NCEP CFS. It is found

that the change of low cloud cover alone has a minor influence on the amount of net shortwave radiation reaching the surface and on the warm biases in the southeastern Atlantic, suggesting that the reflection by low cloud cover plays a secondary role in blocking the radiation in the radiation parameterization of the CFS. Further experiments indicate that the absorption of shortwave radiation by low clouds is mainly determined by CLWP. In the experiments that CLWP is prescribed using observations, the mean climate in the tropics is improved significantly, suggesting that shortwave radiation absorption by the CLWP is mainly responsible for reducing the excessive surface net shortwave radiation over the southern oceans in the CFS. Corresponding to large CLWP values in the southeastern

oceans, the model generates large low cloud amounts. That results in reduction of net shortwave radiation at the ocean surface and the warm biases of SST in the southeastern oceans. Meanwhile, the cold tongue and associated surface wind stress in the eastern oceans become stronger and more realistic. The seasonal cycle in the tropical Atlantic is also improved.

Following on the results from these sensitivity experiments, we conducted an experiment in which the CLWP is prescribed only in the southeastern Atlantic by using annual mean climatology of CLWP. It is shown that the warm biases in the southeastern Atlantic are largely eliminated, and the seasonal cycle in the tropical Atlantic Ocean is significantly improved. Since the change in this experiment is only the annual mean CLWP, it appears that the improvement in the seasonal cycle is a consequence of the improvement in the annual mean tropical climate. It seems that prescribing CLWP in the CFS is an effective interim technique to reduce model biases and to improve the simulation of seasonal cycle in the tropics. This could then serve as a model bias correction approach.

Our work confirms the hypothesis that reduction of low cloud errors may eliminate the warm biases in the southeastern Atlantic Ocean. This is of course only an interim solution to the bias problem, which must eventually be solved by improvement of the model physical parameterizations and dynamics.

Our previous study does show that the low cloud error is originated from the atmospheric component of the CFS (GFS) (see Fig. 12 of Huang et al. 2007). In fact, a comparison of the low cloud simulations by a set of CFS hindcasts with a GFS simulation shows that they have very similar low cloud distribution, with serious deficiency in the southeastern oceans, even though the latter is forced by observed SST. On the other hand, Hu et al. (2008a) compared low cloud amounts in the CFS, ISCCP, and NCEP/ NCAR reanalysis. The model used in the reanalysis is similar to the GFS. It was found that low cloud amount over the southeastern Atlantic in the NCEP/NCAR reanalysis is much closer to ISCCP than to that in the CFS. It suggests that more realistic temperature stratification in the lower troposphere in the NCEP/NCAR reanalysis, due to data assimilation, can improve the low cloud distribution significantly.

References

Clement AC, Burgman R, Norris JR (2009) Observational and model evidence for positive low-level cloud feedback. Science 523(5939):460–464. doi:10.1126/science.1171255

Collins W et al (2006) The Community Climate System Model: CCSM3. J Clim 19:2122–2143

da Silva A, Young CC, Levitus S (1994) Atlas of surface marine data 1994. vol 1: Algorithms and procedures. NOAA Atlas NESDIS 6, US Department of Commerce, Washington, DC, 83 pp

Davey MK et al (2002) STOIC: a study of coupled model climatology and variability in tropical ocean regions. Clim Dyn 18:403–420. doi:10.1007/s00382-001-0188-6

Deser C, Capotondi A, Sravanan R, Phillips AS (2006) Tropical Pacific and Atlantic climate variability in CCSM3. J Clim 19:2451–2481

Gordon CT, Rosati A, Gudgel R (2000) Tropical sensitivity of a coupled model to specified ISCCP low clouds. J Clim 13:2239–2260

Gudgel RG, Rosati A, Gordon CT (2001) The sensitivity of a coupled atmosphericoceanic GCM in prescribed low-level clouds over the ocean and tropical landmasses. Mon Weather Rev 129:2103–2115

Hong S-Y, Pan H-L (1996) Nonlocal boundary layer vertical diffusion in a medium-range forecast model. Mon Weather Rev 124:2322–2339

Hou Y-T, Moorthi S, Campana K (2002) Parameterization of solar radiation transfer in the NCEP models. NCEP Office Note, vol 441, pp 1–46 (available at "http://www.emc.ncep.noaa.gov/officenotes/newernotes/on441.pdf")

Hu Z-Z, Huang B (2007) The predictive skill and the most predictable pattern in the tropical Atlantic: the effect of ENSO. Mon Weather Rev 135(5):1786–1806

Hu Z-Z, Huang B, Pegion K (2008a) Low cloud errors over the southeastern Atlantic in the NCEP CFS and their association with lower-tropospheric stability and air–sea interaction. J Geophys Res (Atmosphere) 113:D12114. doi:10.1029/2007JD 009514

Hu Z-Z, Huang B, Pegion K (2008b) Leading patterns of the tropical Atlantic variability in a coupled GCM. Clim Dyn 30(7/8):703–726. doi:10.1007/s00382-007-0318-x

Hu Z-Z, Huang B, Pegion K (2009) Biases and the most predictable patterns in the NCEP CFS over the tropical Atlantic Ocean. In: Askew ES, Bromley JP (eds) The Atlantic and Indian oceans: new oceanographic research. Nova Science Publishers, Inc., New York, pp 1–15 ISBN: 978-1-60692-475-4

Huang B, Hu Z-Z (2007) Cloud-SST feedback in southeastern tropical Atlantic anomalous events. J Geophys Res (Ocean) 112:C03015. doi:10.1029/2006JC003626

Huang B, Hu Z-Z, Jha B (2007) Evolution of model systematic errors in the tropical Atlantic basin from the NCEP coupled hindcasts. Clim Dyn 28(7/8):661–682. doi:10.1007/s00382-006-0223-8

Kalnay E et al (1996) The NCEP/NCAR 40-year reanalysis project. Bull Am Meteorol Soc 77:437–471

Klein SA, Hartmann DL (1993) The seasonal cycle of low stratiform clouds. J Clim 6:1587–1606

Ma C-C, Mechoso CR, Robertson AW, Arakawa A (1996) Peruvian stratus clouds and the tropical Pacific circulation-A coupled ocean-atmosphere GCM study. J Clim 9:1635–1645

Mechoso CR et al (1995) The seasonal cycle over the tropical Pacific in general circulation models. Mon Weather Rev 123:2825–2838

Mitchell TP, Wallace JM (1992) On the annual cycle in equatorial convection and sea surface temperature. J Clim 5:1140–1156

Neelin JD et al (1992) Tropical air–sea interaction in general circulation models. Clim Dyn 7:73–104

Nigam S (1997) The annual warm to cold phase-transition in the eastern equatorial Pacific: diagnosis of the role of stratus cloud-top cooling. J Clim 10:2447–2467

Norris JR (1998) Low cloud type over the ocean from surface observations. Part II: geographical and seasonal variations. J Clim 11:383–403

O'Dell CW, Wentz FJ, Bennartz R (2008) Cloud liquid water path from satellite based passive microwave observations: a new climatology over the global oceans. J Clim 21:1721–1739

Pacanowski RC, Griffies SM (1998) MOM 3.0 manual. NOAA/ Geophysical Fluid Dynamics Laboratory, Princeton, New Jersey, USA 08542, 668 pp

Philander SGH, Gu D, Halpern D, Lambert G, Lau N-C, Li T, Pacanowski RC (1996) Why the ITCZ is mostly north of the equator. J Clim 9:2958–2972

Rossow WB, Dueñas EN (2004) The International Satellite Cloud Climatology Project (ISCCP) web site: an online resource for research. Bull Am Meteorol Soc 85:167–172

Saha S et al (2006) The NCEP climate forecast system. J Clim 19:3483–3517

Siebesma AP et al (2004) Cloud representation in general-circulation models over the northern Pacific Ocean: a EUROCS intercomparison study. Q J R Meteorol Soc 130:3245–3267

Smith TM, Reynolds RW (2003) Extended reconstruction of global sea surface temperatures based on COADS data (1854–1997). J Clim 16:1495–1510

Tanimoto Y, Xie S-P (2002) Inter-hemispheric decadal variations in SST, surface wind, heat flux and cloud cover over the Atlantic Ocean. J Meteorol Soc Jpn 80:1199–1219

Uppala SM et al (2005) The ERA-40 re-analysis. Q J R Meteorol Soc 131:2961–3012. doi:10.1256/qj.04.176

Wang W, Saha S, Pan H-L, Nadiga S, White G (2005) Simulation of ENSO in the new NCEP coupled forecast system model. Mon Weather Rev 133:1574–1593

Weng F, Grody NC, Ferraro R, Basist Forsyth D (1997) Cloud liquid water climatology from the special sensor microwave/imager. J Clim 10:1086–1098

Wood R, Bretherton CS (2006) On the relationship between stratiform low cloud cover and lower tropospheric stability. J Clim 19:6425–6432

Woodruff SD, Slutz RJ, Jenne RL, Steurer PM (1987) A comprehensive ocean–atmosphere data set. Bull Am Meteorol Soc 68:1239–1250

Wu DL et al (2009) Vertical distributions and relationships of cloud occurrence frequency as observed by MISR, AIRS, MODIS, OMI, CALIPSO, and CloudSat. Geophys Res Lett 36:L09821. doi:10.1029/2009GL037464

Xie S-P (2005) Chapter 4: The shape of continents, air–sea interaction, and the rising branch of the Hadley circulation. In: Diaz HF, Bradley RS (eds) The hadley circulation: present, past and future. Kluwer Academic Publishers, The Netherlands, pp 173–202

Xie P, Arkin PA (1996) Analyses of global monthly precipitation using gauge observations, satellite estimates, and numerical model predictions. J Clim 9:840–858

Xie P, Arkin PA (1997) Global precipitation: a 17-year monthly analysis based on gauge observations, satellite estimates and numerical model outputs. Bull Am Meteorol Soc 78:2539–2558

Xie S-P et al (2007) A regional ocean–atmosphere model for eastern Pacific climate: toward reducing tropical biases. J Clim 20:1504–1522

Xu K-M, Randall DA (1996) A semiempirical cloudiness parameterization for use in climate models. J Atmos Sci 53:3084–3102

Yu J-Y, Mechoso CR (1999) Links between annual variations of Peruvian stratocumulus clouds and of SST in the eastern equatorial Pacific. J Clim 12:3305–3318

Zhang Y, Rossow WB, Lacis AA (2004) Calculation of radiative fluxes from the surface to top of atmosphere based ISCCP and other global data sets: refinements of the radiative transfer model and the input data. J Geophys Res (Atmos) 109. doi:10.1029/2003JD004457